REPORT DOCUMENTATION PAGE

Form Approved OMB NO. 0704-0188

1. REPORT DATE (DD-MM-YYYY)	2. REPORT TYPE	3. DATES COVERED (From - To)
14-05-2018	Final Report	15-Jul-2016 - 14-Feb-2018

4. TITLE AND SUBTITLE
Final Report: Condensed Matter Physics: Topological Heterostructures

5a. CONTRACT NUMBER
W911NF-16-1-0387

5b. GRANT NUMBER

5c. PROGRAM ELEMENT NUMBER
611102

6. AUTHORS

5d. PROJECT NUMBER

5e. TASK NUMBER

5f. WORK UNIT NUMBER

7. PERFORMING ORGANIZATION NAMES AND ADDRESSES
College of William and Mary
P.O. Box 8795

Williamsburg, VA 23187 -8795

8. PERFORMING ORGANIZATION REPORT NUMBER

9. SPONSORING/MONITORING AGENCY NAME(S) AND ADDRESS (ES)
U.S. Army Research Office
P.O. Box 12211
Research Triangle Park, NC 27709-2211

10. SPONSOR/MONITOR'S ACRONYM(S)
ARO

11. SPONSOR/MONITOR'S REPORT NUMBER(S)
69140-PH.4

12. DISTRIBUTION AVAILIBILITY STATEMENT
Approved for public release; distribution is unlimited.

13. SUPPLEMENTARY NOTES
The views, opinions and/or findings contained in this report are those of the author(s) and should not contrued as an official Department of the Army position, policy or decision, unless so designated by other documentation.

14. ABSTRACT

15. SUBJECT TERMS

16. SECURITY CLASSIFICATION OF:			17. LIMITATION OF ABSTRACT	15. NUMBER OF PAGES	19a. NAME OF RESPONSIBLE PERSON
a. REPORT	b. ABSTRACT	c. THIS PAGE			Enrico Rossi
UU	UU	UU	UU		19b. TELEPHONE NUMBER 757-221-3515

RPPR Final Report
as of 14-May-2019

Agency Code:

Proposal Number: 69140PH **Agreement Number: W911NF-16-1-0387**
INVESTIGATOR(S):

Name: Ph.D. Enrico Rossi
Email: erossi@wm.edu
Phone Number: 7572213515
Principal: Y

Organization: **College of William and Mary**
Address: P.O. Box 8795, Williamsburg, VA 231878795
Country: USA
DUNS Number: 074762238 EIN: 546001802
Report Date: 14-May-2018 Date Received: 14-May-2018
Final Report for Period Beginning 15-Jul-2016 and Ending 14-Feb-2018
Title: Condensed Matter Physics: Topological Heterostructures
Begin Performance Period: 15-Jul-2016 **End Performance Period:** 14-Feb-2018
Report Term: 0-Other
Submitted By: Ph.D. Enrico Rossi Email: erossi@wm.edu
Phone: (757) 221-3515
Distribution Statement: 1-Approved for public release; distribution is unlimited.

STEM Degrees: **STEM Participants:** 4

Major Goals: The overall research thrust of the proposed research is the study of heterostructures formed by a system in a topologically nontrivial state and a superconductor. Via the proximity effect the superconductor induces superconducting pairing correlations in the topological material giving rise to novel electronic states with unusual properties. We plan to focus specifically on two types of heterostructures: (i) WSM-superconductor heterostructures, (ii) heterostructures formed by graphene (or bilayer graphene) in the QH regime and a superconductor. The specific objectives of the proposed research are:

Develop the theoretical foundations to describe the electronic properties of WSM-superconductor heterostructures, considering in particular how such properties depend on the topological class to which the WSM belongs and on the symmetries of the superconducting pairing in the superconductor;

Develop a quantitative theory of the proximity effect between the quantum Hall edge states of graphene and a superconductor and in general identify graphene-based structure that would be able to support electronic non-abelian electronic states such as Majorans and, more in general, parafermions;

Understand quantitatively topological the quasi one-dimensional semiconductor/superconductor structures in which signature of Majorana zero modes have been observed;

Understand the role of disorder in topological heterostructures.

Accomplishments: During the course of the project we have developed the theory and the numerical approaches to describe junctions formed by superconductors (SCs) and nodal ring Weyl semimetals (WSMs). In particular, we have focused on developing the theoretical and numerical tools to obtain the Josephson current in SC-WSM-SC junctions. One of the key property of nodal ring WSMs is to have surface states, so called "drumhead states", with an almost flat dispersion (i.e. with a very large effective mass). Such surface states are extremely interesting because they are a clear signature of the nodal ring character of the WSM, they are expected to give rise to anomalous transport properties, and be susceptible to strong correlation effects. We have carefully characterized the nodal rings and the corresponding bands. In real systems it is expected that the drumhead states will have some finite dispersion. We showed how SC-WSM junctions can be used to detect the effective mass (flatness) of the drumhead states. Our results suggest that a measurement of the Andreev reflection can be used to detect the polarization and the effective mass of drumhead states. We then developed the approach to calculate the Josephson current for SC-WSM-SC junctions.

RPPR Final Report
as of 14-May-2019

The ideal 2D nature of graphene and its high mobility make graphene-based heterostructures very promising systems for the realization of ideal topological states able to support Majorana modes and more in general parafermions. One of the limitations of graphene is the lack of significant spin-orbit coupling (SOC). The SOC of graphene can be greatly enhanced via the proximity effect in graphene--topological-insulator (TI) heterostructures. We have obtained the current-spin response of graphene-TI heterostructures and shown that this response is much larger in these heterostructures than in TIs alone. In particular we have found that such response is very large in heterostructures formed by bilayer graphene and a TI in the tetradymite family.

Quasi 1D confinement favors the establishment of superconducting topological phases with Majorana modes. This fact motivated us to consider the possibility to use graphene nanoribbons (GNR) as a platform to realize Majorana states given their quasi 1D nature and potentially high mobility. As for graphene, however, GNRs have very small SOC. To enhance the SOC in GNRs we have studied the effect of placing them in proximity of a monolayer of a transition metal dichalcogenide (TMD) in which the SOC is very strong. Due to the large mismatch between graphene and TMDs we first had to identify the GNR-TMD structures that minimize strain. For these structure using density functional theory we obtained the band structure and the spin-dependent splitting of the bands due to SOC. In the last part of the project we have completed this study by considering the case of NbSe2. NbSe2 is a special TMD because it becomes superconducting at low temperature. In addition, the strong SOC induces an Ising superconducting pairing that makes superconductivity in NbSe2 very robust against in-plane magnetic fields: the superconducting pairing survives for magnetic fields an order of magnitude larger than the one corresponding to the Pauli limit. These facts make GNR-NbSe2 heterostructures very promising for the realization of Majorana modes.

Heterostructures based on graphene layers in the quantum Hall regime and superconductors are expected to be able to support parafermions. In realistic conditions the graphene layers could be in FQHS with different filling factor "nu". For this reason we have generalized the construction of the parafermion operators to the case when the graphene layers have filling factors that are different. We have found the commutation relation for the parafermion operators for this case. Motivated by the recent experimental observation of chiral Majorana modes in quantum anomalous Hall (QAH) systems we have recently realized that the non-abelian states that can be realized in graphene FQHS systems can be most easily probed using similar setups to the ones recently used to probe the chiral Majoranas in QAH systems. The project has then evolved to understand this type of setup.

We have developed a theoretical and numerical approach to obtain the electronic properties and the topological phase diagram of semiconductor-SC (SM-SC) nanowires taking into account the presence of gate-induced electric fields, fields that are using experimentally to control the phase (topological or trivial) of the wire and to perform various measurements. The approach we developed is based on the self-consistent solution of the Schrodinger-Poisson equations. We have been able to understand the conditions necessary to achieve a strong coupling regime between the SC and the SM. We have found that the band bending "W" at the interface between the SM and the SC plays an essential role in determining the strength of the hybridization between SM and SC. The main results of this work are: (i) Full topological phase diagram as a function of magnetic field "B" and external gate voltage; (ii) Dependence of the system's g-factor on the external gate voltage. This result is important because it explains the decrease of the range of values of B for which the system is in the topological phase as the coupling between the SM and the SC increases. One important outcome of our work is that it shows that the optimal operating regime to realize Majorana states in SM-SC heterostructures in general is not the one that maximizes the induced gap given that an increase of the induced gap is associated with a decrease of the effective g-factor. For each SM-SC heterostructure there is an optimal hybridization strength that maximizes the region in parameter's space for which the system is in the topological phase supporting Majorana modes.

The unavoidable presence of impurities in SM-SC heterostructure can significantly affect the realization and manipulation of Majorana modes. In the most recent experimental devices the SM and the SM/SC interface are of very high quality and expected to have a very low density of impurities. However, the SC itself and the top surface of the SC are expected to have a non negligible number of defects. For this reason we have studied the issue of ``if'' and ``how'' defects in the SC alone can affect the realization and observation of Majorana modes in SM-SC heterostructures. Given that no magnetic impurities are expected to be present, we considered the case in which the impurities are scalar. We have obtained the general formalism to address the problem of a single impurity in SC-based heterostructures and studied in detail the case of quasi 1D nanowires formed by a SC and SM with SOC. We have found that, due the interplay between tunneling and scattering processes in these structure we can have impurity-induced bound states even when the SC is purely s-wave. In addition we found that the ratio between the Fermi wave vector of the SM, and the Fermi wave vector of the SC largely controls if the impurity bound states will occur in the topological or trivial phase of the nanowire. The other key parameters are Zeeman

splitting and the SM-SC coupling strength. The results of this part of the project provide guidance for the optimization of superconductor-semiconductor heterostructures: although a strong tunneling is beneficial to obtain a large gap it also enhances the effect of the impurities located in the s-wave superconductor on the superconducting state induced in the semiconductor. Therefore, we find that, when the effect of impurities is included, the optimal coupling to the superconductor is not strong but intermediate.

Training Opportunities: During the course of the project a Graduate student was involved and supported full time by the grant and received training in the field of condensed matter via one-on-one meetings with the PI and group meetings with other members of the PI's group. Two other graduate students have been involved with the project and have received partial support.

An undergraduate was involved in the research but not supported directly by the grant, and received training in the physics and condensed matter via one-on-one meetings.

Results Dissemination: An article has been published in Physical Review B, rapid communications.

An article has been published in Physical Review B.

A manuscript has been posted on the arXiv and is currently under review at Phys. Rev. X.

Five contributed talks based on the research carried out during the project have been presented at the 2018 APS March Meeting.

Results obtained during the project have been presented at the Spring 2018 "Q-Meeting", Station-Q, Santa Barbara CA (March 2018).

Results obtained during the project have been presented at the Spring 2017 "Q-Meeting", Station-Q, Santa Barbara CA (June 2017).

Results obtained during the project have been presented at the "Majorana states in condensed matter: towards topological quantum computation" conference, Institute for Cross-Disciplinary Physics and Complex Systems, Mallorca Spain (May 2017).

Results obtained during the project have been presented at the Spring 2017 "Numerics Meeting", Niels Bohr Institute, Copenhagen, Denmark (May 2017).

Results obtained during the project have been presented at the 2017 APS March meeting in contributed talks, New Orleans LA (March 2017).

Results obtained during the project have been presented at the "Topological States of Matter Conference", International Institute of Physics, Natal, Brazil (March, 2017).

The PI has given a Colloquium presenting results obtained during the project at the University of Texas at Dallas (September 2016).

The PI has given an invited talk presenting results obtained during the project at Radboud University, Nijmegen The Netherlands (October 2016).

Results obtained during the project have been presented at the Fall 2016 "Numerics Meeting", TU Delft, Delft The Netherlands (October 2016).

Results obtained during the project have been presented at the Fall 2016 "Q-Meeting", Station-Q, Santa Barbara CA (December 2016).

The PI has given an invited talk presenting results obtained during the project at the "The electronic and optical properties of 2D and Dirac Materials Workshop", Jacksonville FL (December 2016)

Honors and Awards: The PI received the "Plumeri Award" for Faculty Excellence (William & Mary).

RPPR Final Report
as of 14-May-2019

Protocol Activity Status:

Technology Transfer: Nothing to Report

PARTICIPANTS:

Participant Type: PD/PI
Participant: Enrico Rossi
Person Months Worked: 1.00 **Funding Support:**
Project Contribution:
International Collaboration:
International Travel:
National Academy Member: N
Other Collaborators:

Participant Type: Graduate Student (research assistant)
Participant: Jiani Lu
Person Months Worked: 12.00 **Funding Support:**
Project Contribution:
International Collaboration:
International Travel:
National Academy Member: N
Other Collaborators:

Participant Type: Graduate Student (research assistant)
Participant: Christopher Hipp
Person Months Worked: 2.00 **Funding Support:**
Project Contribution:
International Collaboration:
International Travel:
National Academy Member: N
Other Collaborators:

Participant Type: Graduate Student (research assistant)
Participant: Yohanes Gani
Person Months Worked: 1.00 **Funding Support:**
Project Contribution:
International Collaboration:
International Travel:
National Academy Member: N
Other Collaborators:

ARTICLES:

RPPR Final Report
as of 14-May-2019

Publication Type: Journal Article Peer Reviewed: Y **Publication Status:** 1-Published
Journal: Physical Review B
Publication Identifier Type: DOI Publication Identifier: https://doi.org/10.1103/PhysRevB.96.235419
Volume: 96 Issue: First Page #: 235419
Date Submitted: 5/11/18 12:00AM Date Published: 12/13/17 5:00AM
Publication Location:
Article Title: Giant Edelstein effect in topological-insulator–graphene heterostructures
Authors: M. Rodriguez-Vega, G. Schwiete, J. Sinova, E. Rossi
Keywords: graphene, spin, topological insulator
Abstract: The control of a ferromagnet's magnetization via only electric currents requires the efficient generation of current-driven spin torques. In magnetic structures based on topological insulators (TIs) current-induced spin-orbit torques can be generated. Here we show that the addition of graphene, or bilayer graphene, to a TI-based magnetic structure greatly enhances the current-induced spin-density accumulation and significantly reduces the amount of power dissipated. We find that this enhancement can be as high as a factor of 100, giving rise to a giant Edelstein effect. Such a large enhancement is due to the high mobility of graphene (bilayer graphene) and to the fact that the graphene (bilayer graphene) sheet very effectively screens charge impurities, the dominant source of disorder in topological insulators. Our results show that the integration of graphene in spintronics devices can greatly enhance their performance and functionalities.
Distribution Statement: 1-Approved for public release; distribution is unlimited.
Acknowledged Federal Support: **Y**

Publication Type: Journal Article Peer Reviewed: Y **Publication Status:** 1-Published
Journal: Physical Review B
Publication Identifier Type: DOI Publication Identifier: 10.1103/PhysRevB.97.161408
Volume: 97 Issue: 16 First Page #: 161408(R)
Date Submitted: 5/11/18 12:00AM Date Published: 4/26/18 8:00AM
Publication Location:
Article Title: Impurity-induced states in superconducting heterostructures
Authors: Dong E. Liu, Enrico Rossi, Roman M. Lutchyn
Keywords: Superconductor, impurity, topological materials, Majorana
Abstract: Heterostructures allow the realization of electronic states that are difficult to obtain in isolated uniform systems. Exemplary is the case of quasi-one-dimensional heterostructures formed by a superconductor and a semiconductor with spin-orbit coupling in which Majorana zero-energy modes can be realized. We study the effect of a single impurity on the energy spectrum of superconducting heterostructures. We find that the coupling between the superconductor and the semiconductor can strongly affect the impurity-induced states and may induce additional subgap bound states that are not present in isolated uniform superconductors. For the case of quasi-one-dimensional superconductor/semiconductor heterostructures we obtain the conditions for which the low-energy impurity-induced bound states appear.
Distribution Statement: 1-Approved for public release; distribution is unlimited.
Acknowledged Federal Support: **Y**

RPPR Final Report
as of 14-May-2019

Publication Type: Journal Article Peer Reviewed: N **Publication Status:** 4-Under Review
Journal: arXiv
Publication Identifier Type: Other Publication Identifier: eprint arXiv:1801.02616
Volume: Issue: First Page #:
Date Submitted: 5/11/18 12:00AM Date Published: 1/8/18 5:00AM
Publication Location:
Article Title: Effects of gate-induced electric fields on semiconductor Majorana nanowires
Authors: Andrey E. Antipov, Arno Bargerbos, Georg W. Winkler, Bela Bauer, Enrico Rossi, Roman M. Lutchyn
Keywords: Superconductor, topological materials, Majorana, semiconductor, nanowire
Abstract: We study the effect of gate-induced electric fields on the properties of semiconductor-superconductor hybrid nanowires which represent a promising platform for realizing topological superconductivity and Majorana zero modes. Using a self-consistent Schrodinger-Poisson approach that describes the semiconductor and the superconductor on equal footing, we are able to access the strong tunneling regime and identify the impact of an applied gate voltage on the coupling between semiconductor and superconductor. We discuss how physical parameters such as the induced superconducting gap and Land\'e g-factor in the semiconductor are modified by redistributing the density of states across the interface upon application of an external gate voltage. Finally, we map out the topological phase diagram as a function of magnetic field and gate voltage for InAs/Al nanowires.

Acknowledged Federal Support: **Y**

Topological heterostructures
W911NF-16-1-0387

Enrico Rossi
Physics Department, William & Mary, Williamsburg, VA 23187.

During the course of the project we have developed the theory and the numerical approaches to describe junctions formed by superconductors (SCs) and nodal ring Weyl semimetals (WSMs). In particular, we have focused on developing the theoretical and numerical tools to obtain the Josephson current in SC-WSM-SC junctions. One of the key property of nodal ring WSMs is to have surface states, so called *drumhead states*, with an almost flat dispersion (i.e. with a very large effective mass). Such surface states are extremely interesting because they are a clear signature of the nodal ring character of the WSM, they are expected to give rise to anomalous transport properties, and be susceptible to strong correlation effects. We have three possible situations in which the nodal ring, Fig. 1 (a), is preserved:

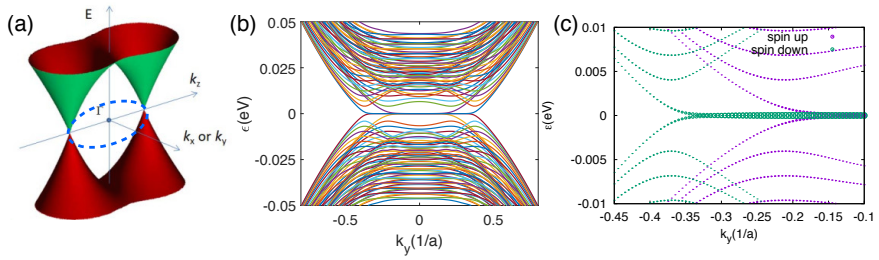

Figure 1: (a) Sketch of low energy Fermi surface of a nodal ring WSM. (b) Band structure of a nodal ring WSM in which spin-rotation and time reversal symmetry are broken. (c) Detail of (b) that shows that, due to the reduced symmetry, for $k_y \lesssim -0.2/a$ some of the surface states merge into the bulk bands. The different color denote different spin polarizations.

i. fully symmetric case for which the ring is fourfold degenerate;
ii. spin-rotation and time reversal symmetry broken case in which the ring is splitted into two twofold degenerate rings;
iii. spin-rotation and inversion symmetry broken case in which the ring is also splitted into two twofold degenerate rings.

We have carefully characterized the nodal rings and the corresponding bands of cases (ii) and (iii). Fig. 1 (b) show the spectrum of a finite thickness slab of a nodal ring WSM in which both the spin-rotation and time reversal symmetry have been broken (case (ii)). The zoomed-in plot of Fig. 1 (c) shows how, as consequence of the lowered symmetry, some of the surface states that are degenerate in case (i) start merging with the bulk states. In addition it shows the spin polarization of the states. A symmetry analysis of the surface states allows us to identify which of the surface states are expected to be robust, i.e. insensitive to local perturbations. The combination of such symmetry analysis with the type of results shown in Fig. 1 allows the identification of which states will pair via the proximity effect due to the presence of a

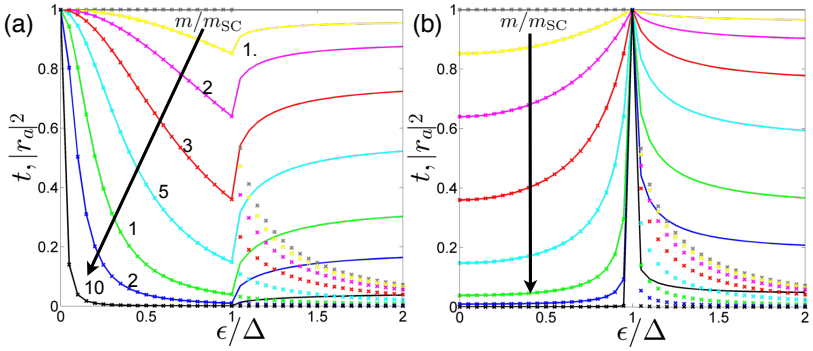

Figure 2: (a) Magnitude of the Andreev reflection, $|r_a|^2$, as a function of the quasiparticle energy ϵ for a junction between an s-wave SC and the surface of a nodal ring WSM with unpolarized drumhead states. (b) Magnitude of the Andreev reflection, $|r_a|^2$, as a function of the quasiparticle energy ϵ for a junction between a p-wave SC and the surface of a nodal ring WSM with spin-polarized drumhead states.

superconductor placed on the surface of the WSM.

In Fig. 1 (b) the surface states are assumed to have a completely flat surface. However, in real systems it is expected that such states will have some finite dispersion. We showed how SC-WSM junctions can be used to detect the effective mass (flatness) of the drumhead states. For this purpose we have obtained the transmission and reflection coefficients for SC-WSM junction as a function of the ratio, $m/m_{\rm SC}$, between the effective mass (m) of the drumhead states and the one ($m_{\rm SC}$) of the quasiparticles in the SC. Fig. 2 (a) shows how the square of the Andreev reflection, $|r_a|^2$, depends on the energy ϵ of the quasiparticle scattering at the interface for case (i) with s-wave pairing in the SC. We see that $|r_a|^2$ decreases as $m/m_{\rm SC}$ increases. In Fig. 2 (b) we show the results for the case in which the drumhead states are assumed to be spin-polarized, to mimic case (ii), and the pairing in the SC is p-wave. The overall behavior is very different from the one shown in Fig. 2 (a) but we still find that $|r_A|^2$ decreases as $m/m_{\rm SC}$ increases (apart from the case when ϵ is equal to the SC gap Δ). These results suggest that a measurement of $|r_A|^2$ can be used to detect the polarization and the effective mass of drumhead states.

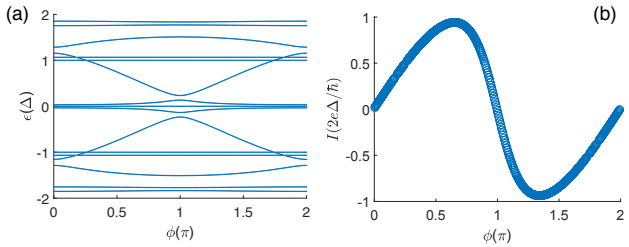

Figure 3: (a) Spectrum of Andreev bound states as a function of ϕ for a SC-WSM-SC junction assuming p-wave pairing in the SC and realistic dispersion for the WSM including both surface and bulk states (limit $W \to 0$). $\mu = 1.32\Delta$. (b) Josephson current I as function of ϕ corresponding to spectrum shown in (a).

We then developed the approach to calculate the Josephson current for SC-WSM-SC junctions. The approach adapts to the case of SC-WSM-SC junctions the theory that was developed to relate the Josephson current of SC-N-SC junctions (where N denotes a normal metal) to the scattering matrix of the normal region N. This approach is very effective and allows to take into account efficiently the finite width, W, of the junction. We have obtained results for finite width junctions. To be able to understand these results and relate them to the properties of the drumhead states, we studied in detail the case when $W \to 0$ for a which it is possible to carry out a semi-analytical treatment. Figure 3 (a) shows how the spectrum of a finite size SC-WSM-SC junctions evolves as a function of the phase difference ϕ between the two superconductors. The low energy states are Majorana modes arising from the p-wave nature of the SCs. The higher energy subgap states that don't disperse with ϕ are WMS's bulk states. Figure 3 (b) shows the Josephson current corresponding to the spectrum shown in Fig. (a).

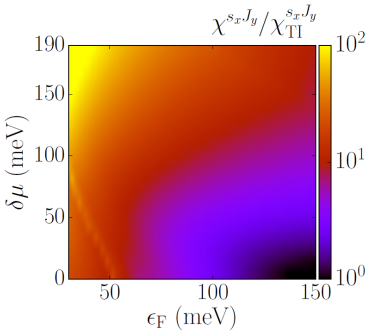

Figure 4: Ratio between the current-spin response $\chi^{s_x J_y}$ of a bilayer-graphene–TI heterostructure and the current-spin response $\chi_{\rm TI}^{s_x J_y}$ of an isolated TI as a function of the Fermi energy ϵ_F and of the band mismatch $\delta\mu$ between the TI and bilayer graphene.

The ideal 2D nature of graphene and its high mobility make graphene-based heterostructures very promising systems for the realization of ideal topological states able to support Majorana modes and more in general parafermions. One of the limitations of graphene is the lack of significant spin-orbit coupling (SOC). The SOC of graphene can be greatly enhanced via the proximity effect in graphene–topological-insulator (TI) heterostructures. We have obtained the current-spin response of graphene-TI heterostructures and shown that this response is much larger in these heterostructures than in TIs alone. In particular we have found that such response is very large in heterostructures formed by bilayer graphene and a TI in the tetradymite family (such as Sb_2Te_3, Bi_2Se_3 and Bi_2Te_3) as shown in Fig. 4.

Quasi 1D confinement favors the establishment of superconducting topological phases with Majorana modes. This fact motivated us to consider the possibility to use graphene nanoribbons (GNR) as a platform to realize Majorana states given their quasi 1D nature and potentially high mobility. As for graphene, however, GNRs have very small SOC. To enhance the SOC in GNRs we have studied the effect of placing them in proximity of a monolayer of a transition metal dichalcogenide (TMD) in which the SOC is very strong. Due to the large mismatch between graphene and TMDs we first had to identify the GNR-TMD structures that minimize strain. For these structure using density functional theory we obtained the band structure and the spin-dependent splitting of the bands due to SOC. In the last part of the project we have completed this study by considering the case of $NbSe_2$. $NbSe_2$ is a special TMD because it becomes superconducting at low temperature. In addition, the strong SOC induces an Ising superconducting pairing that makes superconductivity in $NbSe_2$ very robust against in-plane magnetic fields: the superconducting pairing survives for magnetic fields an order of magnitude larger than the one corresponding to the Pauli limit. These facts make GNR-$NbSe_2$ heterostructures very promising for the realization of Majorana modes. Fig. 5 (a) shows an example of the GNR-TMD structures considered. Fig. 5 (b) shows how the 1D Brillouin Zone (BZ), shown by the small red segments, of a typical GNR intersects the Fermi surfaces of $NbSe_2$ despite the large lattice mismatch. Fig. 5 (c), (d) show the density of states (DOS) for a GNR proximitized to $NbSe_2$ when the in-plane magnetic field $B_{\|}$ is zero, (c), and when $B_{\|}$ is equal to the critical value that drives the GNR into the topological phase.

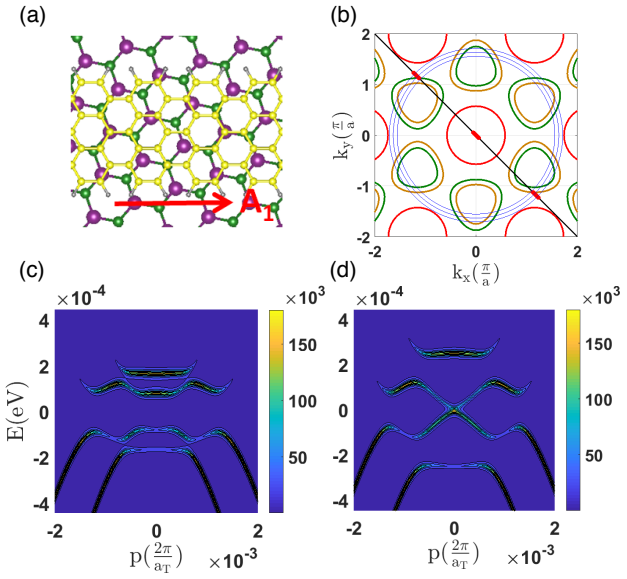

Figure 5: (a) Heterostructure formed by an armchair graphene nanoribbon (GNR) and a monolayer of $MoSe_2$. (b) Overlap between GNR's BZ (red segment on diagonal line) and Fermi surfaces of $NbSe_2$. (c) DOS of GNR on $NbSe_2$ for $B_{\|} = 0$. (d) DOS of GNR on $NbSe_2$ for when $B_{\|}$ is equal to the critical value to drive the GNR into the topological phase.

Heterostructures based on graphene layers in the quantum Hall regime and superconductors, such as the one shown in Fig. 6, are expected to be able to support parafermions. In realistic conditions the graphene layers, shown in red in Fig. 6, could be in FQHS with different filling factor ν. For this reason we have generalized the construction of the parafermion operators (α_i) to the case when the top layer and the bottom layer of Fig. 6 have filling factors ν and ν' that are different. We find that when ν and ν' are different the parafermion operators obey the following commutation relation

$$\alpha_i \alpha_j = \alpha_j \alpha_i e^{i\frac{2\pi}{m^2}[m+m'+\frac{1}{2}(m-m')]\mathrm{sgn}(j-i)}$$

where $m = 1/\nu$ ($m' = 1/\nu'$) and therefore can still describe a non-abelian ground state. Motivated by the recent experimental observation of chiral Majorana modes in quantum anomalous Hall (QAH) systems we have recently realized that the non-abelian states that can be realized in graphene FQHS systems can be most easily probed using similar setups to the ones recently used to probe the chiral Majoranas in QAH systems. The project has then evolved to understand this type of setup.

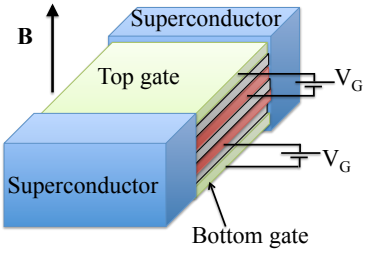

Figure 6: Sketch of graphene-based heterostructure in which parafermions can be realized.

We have developed a theoretical and numerical approach to obtain the electronic properties and the topo-

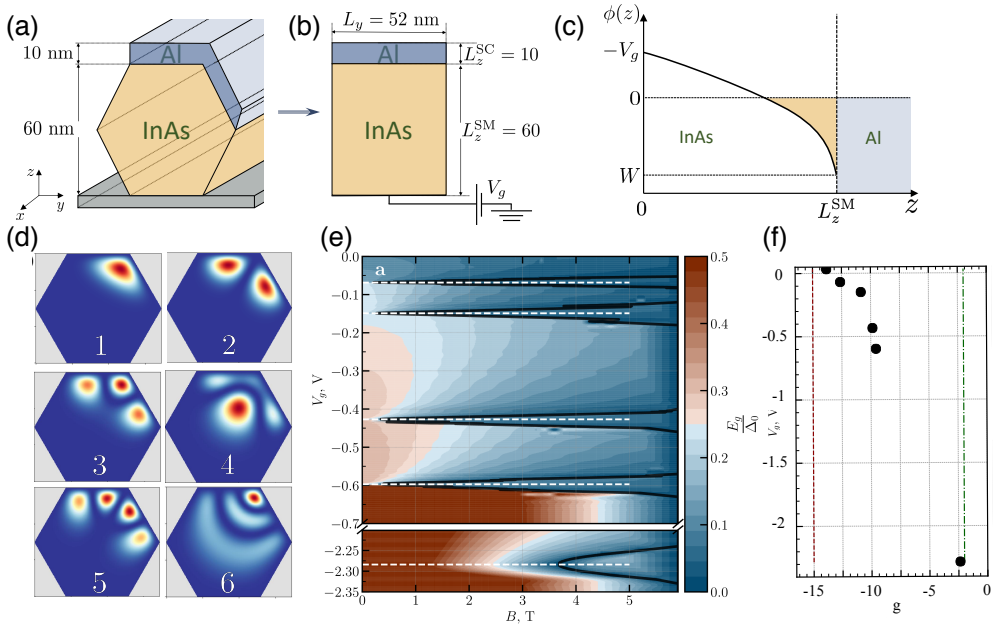

Figure 7: (a) Sketch of geometry of SM-SC nanowire. (b) Sketch of the effective 2D model for SM-SC nanowire. (c) Diagram showing the electrostatic potential in the SM taking into account the band-bending W at the SM-SC interface. (d) Electronic modes below the Fermi energy in the SM. (e) Topological phase diagram in the the (B, V_g) plane and magnitude of the spectral gap. The boundaries of the topological phase are marked with solid black lines. (f) Dependence of the g-factor on the gate voltage V_g.

logical phase diagram of semiconductor-SC (SM-SC) nanowires, see Fig. 7 (a), (b), taking into account the presence of gate-induced electric fields, fields that are using experimentally to control the phase (topological or trivial) of the wire and to perform various measurements. The approach we developed is based on the self-consistent solution of the Schrödinger-Poisson equations. The problem is computationally challenging because the SC is typically a metal (such as Al) with a very large Fermi energy, much larger than the SM's Fermi surface. However, we have been able to overcome these difficulties in part taking advantage of the approximate symmetries of the problem: we first obtained the approximate electronic modes in the fully 3D geometry, see Fig. 7 (d), and then we used this information to obtain an effective 2D model, Fig. 7 (b), that requires much less computational resources to model. We have been able to understand the conditions necessary to achieve a strong coupling regime between the SC and the SM. We have found that the band bendin W at the interface between the SM and the SC, Fig.. 7 (c), plays an essential role in determining the strength of the hybridization between SM and SC and therefore the magnitude of the superconducting gap induced (Δ_{ind}) in the SM, see. The main results of this work are:

1. Full topological phase diagram as a function of magnetic field B *and* external **gate voltage**, V_g, Fig. 7 (e). Previous works obtained the topological phase diagram as a function of B and the chemical potential μ in the SM. However, experimentally what is tuned is V_g, not μ, and V_g, by strongly affecting the hybridization, modifies not just μ but also other parameters of the system such as the g-factor.
2. Dependence of the system's g-factor on the external gate voltage V_g, Fig. 7 (f). This result is important because it explains the decrease of the range of values of B for which the system is in the topological phase, see Fig. 7 (e), as the coupling between the SM and the SC increases (corresponding to large negative values of V_g).

One important outcome of our work is that it shows that the optimal operating regime to realize Majorana states in SM-SC heterostructures in general is not the one that maximizes Δ_{ind} given that an increase of Δ_{ind} is associated with a decrease of the effective g-factor. For each SM-SC heterostructure there is an optimal hybridization strength that maximizes the region in parameter's space for which the system is in the topological phase supporting Majorana modes.

The unavoidable presence of impurities in SM-SC heterostructure can significantly affect the realization and manipulation of Majorana modes. In the most recent experimental devices the SM and the SM/SC interface are of very high quality and expected to have a very low density of impurities. However, the SC itself and the top surface of the SC are expected to have a non negligible number of defects. For this reason we have studied the issue of "if" and "how" defects in the SC alone can affect the realization and observation of Majorana modes in SM-SC heterostructures. Given that no magnetic impurities are expected to be present, we considered the case in which the impurities are scalar. We have obtained the general formalism to address the problem of a single impurity in SC-based heterostructures and studied in detail the case of quasi 1D nanowires formed by a SC and SM with SOC. We have found that, due the interplay between tunneling and scattering processes in these structure we can have impurity-induced bound states even when the SC is purely s-wave. In addition we found that the ratio between the Fermi wave vector of the SM, $k_{F,N}$, and the Fermi wave vector of the SC, $k_{F,SC}$, largely controls if the impurity bound states will occur in the topological or trivial phase of the nanowire. The other key parameters are Zeeman splitting V_x and the SM-SC coupling strength Γ_t. Figure 8 (a) shows in grey-blue (yellow) the regions in the (V_x, Γ_t) plane for which there exist a finite value of impurity strength $u_{\rm imp}$ such that the energy of the bound state is equal to zero ($< 0.6\Delta_{\rm ind}$). The red dashed line shows the boundary between trivial and topological regimes. As the ratio $k_{F,\rm N}/k_{F,\rm SC}$ increases the area where $\omega^* = 0$ decreases in the trivial phase and increases in the topological phase, as shown by Fig. 8 (b). Figure 8 (c), (d) show the evolution of the energy of the impurity-induced bound state for a fixed value of $u_{\rm imp}$ and two different values of the ratio $k_{F,\rm N}/k_{F,\rm SC}$. The results of this part of the project provide guidance for the optimization of superconductor-semiconductor heterostructures: although a strong tunneling is beneficial to obtain a large gap it also enhances the effect of the impurities located in the s-wave superconductor on the superconducting state induced in the semiconductor. Therefore, we find that, when the effect of impurities is included, the optimal coupling to the superconductor is not strong but intermediate, i.e. $\Gamma_t \sim \Delta_0$.

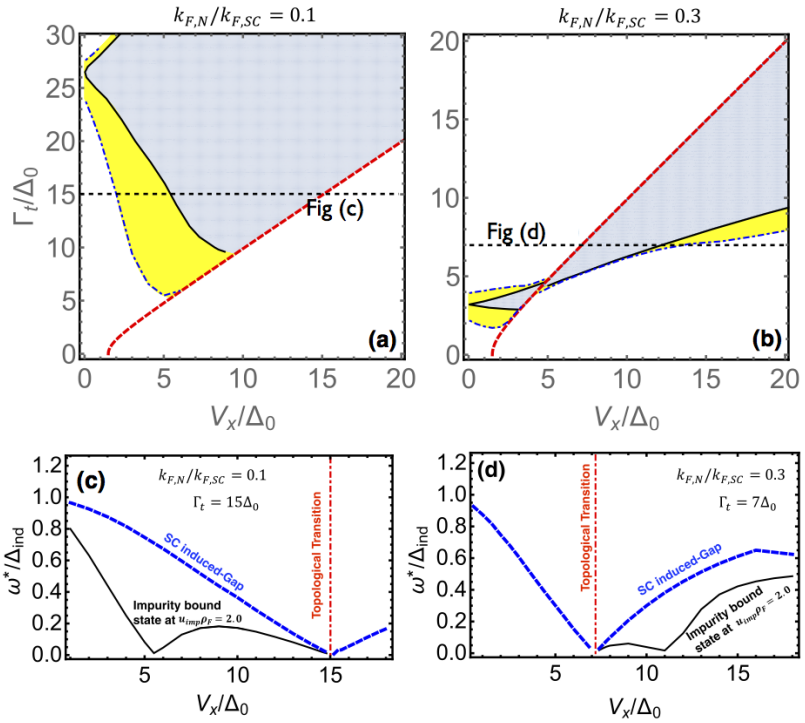

Figure 8: (a) Phase diagram in the (V_x, Γ_t) plane identifying the regions, shown in grey, for which there exist a finite value of $u_{\rm imp}$ such that $\omega^* = 0$. $k_{F,\rm N}/k_{F,\rm SC} = 0.1$. Here the strength of the SOC, $\alpha_{\rm SOC}$, is such that $\alpha_{SOC}k_{F,SC} = 4.2\Delta_0$ where $k_{\rm F,SC}$ is the Fermi wave-vector in the SM with $\mu = 1.5\Delta_0$, and Δ_0 is the gap of the SC. The red dashed line shows the boundary between the trivial and the topological phases. The dot-dash lines identify the boundaries of the yellow regions where $\omega^* < 0.6\Delta_{\rm ind}$, where $\Delta_{\rm ind}$ is the induced gap in the SM. The horizontal dash line is placed at the value of Γ_t for which the results shown in (c) were obtained. (b) Same as (a) but for $k_{F,\rm N}/k_{F,\rm SC} = 0.3$. (c) Spectrum of impurity-induced bound states as a function of the Zeeman splitting V_x for fixed $u_{\rm imp}$. All unspecified parameters values are the same as in Fig. (a). (d) Spectrum of impurity-induced bound states as a function of the Zeeman splitting V_x for fixed $u_{\rm imp}$. All unspecified parameters values are the same as in Fig. (b).